Physica E 74 (2015) 160–167

Contents lists available at ScienceDirect

Physica E

journal homepage: www.elsevier.com/locate/physe

Magnetoresistance oscillations of two-dimensional electron systems in lateral superlattices with structured unit cells

Rolf R. Gerhardts

Max-Planck-Institut für Festkörperforschung, Heisenbergstrasse 1, D-70569 Stuttgart, Germany

HIGHLIGHTS

- Recently observed modulation-induced magnetoresistance oscillations of 2D electron systems are explained.
- The harmonics of the modulation potential, which are relevant for the resistance oscillations, are determined.
- Characteristic differences between electrostatically generated and strain-mediated modulations are emphasized.
- Different types of experiments are explained with the same, well-established formalism.

ARTICLE INFO

Article history:
Received 12 May 2015
Received in revised form
23 June 2015
Accepted 25 June 2015
Available online 2 July 2015

Keywords:
Magnetotransport
Two-dimensional electron systems
Lateral superlattice
Weiss oscillations

ABSTRACT

Model calculations for commensurability oscillations of the low-field magnetoresistance of two-dimensional electron systems (2DES) in lateral superlattices, consisting of unit cells with an internal structure, are compared with recent experiments. The relevant harmonics of the effective modulation potential depend not only on the geometrical structure of the modulated unit cell, but also strongly on the nature of the modulation. While higher harmonics of an electrostatically generated surface modulation are exponentially damped at the position of the 2DES about 90 nm below the surface, no such damping appears for strain-induced modulation generated, e.g., by the deposition of stripes of calixarene resist on the surface before cooling down the sample.

1. Introduction

The calculations presented here are motivated by recent magnetoresistance experiments [1,2] on two-dimensional electron systems (2DES) in $Al_xGa_{1-x}As$-heterostructures with a special type of periodic surface modulation. The modulation of the 2DES, located 90 nm below the sample surface, was achieved by depositing a periodic array of identical, parallel metal stripes, with three stripes per unit cell, onto the sample surface. The three stripes of width a within each unit cell were arranged in such a way, that the distance between neighboring stripes changes periodically from a over $2a$ to $3a$, so that a superlattice of period $A=9a$ with broken inversion symmetry results. Since such samples show interesting transport properties under electro-magnetic irradiation [1,3–5], it seemed interesting to investigate also their quasi-static magnetotransport properties. Indeed, at sufficiently low temperatures and magnetic fields, commensurability oscillations of the magnetoresistance were found, less pronounced but similar to the well-known Weiss oscillations observed on a 2DES with a simple harmonic modulation [6–8].

Conceptually the type of lateral superlattices generated in this way has some similarities with "hyperlattices", which have been investigated some time ago [9] and show also interesting magnetotransport oscillations. These hyperlattices were produced by depositing identical arrays of p parallel stripes of calixarene resist ($p=3$ or 4) with equal center-distances b close to each other onto the surface of an $Al_xGa_{1-x}As$ -heterostructure. The arrays were periodically arranged with a distance qb between neighboring arrays, so that a hyperlattice of stripes with period $A=(p+q)b$ was formed. At low temperatures this caused strain in the semiconductor and, probably via piezoelectric effects, a periodic modulation of the 2DES, which was 90 nm underneath the surface. We will show that both types of experiments can be described by the same formalism.

A 2DES of density n_s in the x–y plane, with a harmonic potential modulation $V_{\rm eff}(x) \propto \cos(2\pi x/A)$ of period A in the x-direction, shows under a homogeneous magnetic field B in z-direction B-dependent Weiss oscillations of the component ρ_{xx} of the

E-mail address: R.Gerhardts@fkf.mpg.de

http://dx.doi.org/10.1016/j.physe.2015.06.027

resistance tensor with minima, if the cyclotron radius $R_c = \hbar\sqrt{2\pi n_s}/(eB)$ at the Fermi energy $E_F = \pi\hbar^2 n_s/m$ (with m being the effective mass of GaAs and $-e$ the electron charge) and the period A satisfy the commensurability condition [6–8]

$$2R_c/A = \lambda - 1/4 \quad \text{for} \quad \lambda = 1, 2, 3, \ldots. \tag{1}$$

This has been explained by quantum-mechanical calculations [7,8,10,11], which show that the modulation-induced broadening of Landau energy levels to Landau bands leads to vanishing band width if Eq. (1) holds, but also by purely classical considerations of the modulation-induced guiding center drift of cyclotron orbits [12].

The resistance correction caused by a periodic modulation with broken inversion symmetry shows also minima at certain values of the applied magnetic field B, but these B-values do not follow a simple commensurability relation between cyclotron diameter $2R_c$ and modulation period A [1]. This is not surprising, since the modulation with broken inversion symmetry introduces a periodic potential containing many harmonics, which yield oscillating contributions with different periods to the resistance. A theoretical approach, decomposing the modulation potential into its Fourier components and adding their contributions to the resistance correction, has been published a long time ago [13]. The basic assumption of this approach is that the modulation is weak enough, so that interactions between different Fourier components can be neglected.

Below we will follow this approach [13] and take into account that the relevance of the Fourier components of a purely electrostatic modulation potential in the surface plane is determined by exponential damping effects, required by Poisson's equation, and by electrostatic screening, which we describe by Lindhard's dielectric constant. We demonstrate that due to these effects, as already mentioned in [1], rather different surface potentials, e.g. those with step-like or smooth peaks, can lead to very similar magnetoresistance oscillations, whereas already slightly different peak-positions in the unit cells may lead to strong modifications of these oscillations.

We also apply the formalism of [13] to the case of "hyperlattices" investigated experimentally by Endo and Iye [9], who explained some of their results within the classical guiding center picture, but did not present a numerical description of the measured magnetoresistance oscillations. We find nice agreement of our calculated and their measured results, but only if we neglect the exponential damping of higher Fourier components, required by Poisson's equation. This seems reasonable, since Endo and Iye emphasize, that their modulation procedure introduces strain, which couples to the 2DES by piezoelectric effects and not by a simple electrostatic surface potential.

2. Model and formalism

In view of the experiments [1,9] we assume a 2DES of density $n_s \sim 2\times 10^{11}\,\mathrm{cm}^{-2}$ in a $Al_xGa_{1-x}As$-heterostructure in the plane $z = d = 90$ nm below the sample surface at $z=0$. In both experiments the unit cells of the periodic array consist of a few parallel stripes, with varying distances between neighboring stripes. We assume that a stripe of width a located at $x = x_0$ and $z=0$ produces in the surface an electrostatic potential $V_{str}(x - x_0, 0)$, which is translation invariant in the y-direction and vanishes for $|x - x_0| > a$. Two stripe-models will be considered, a step potential $V_{str}(x, 0) = V^s(x)$ and a continuous potential $V_{str}(x, 0) = V^c(x)$, both with the same maxima and the same average values, given by

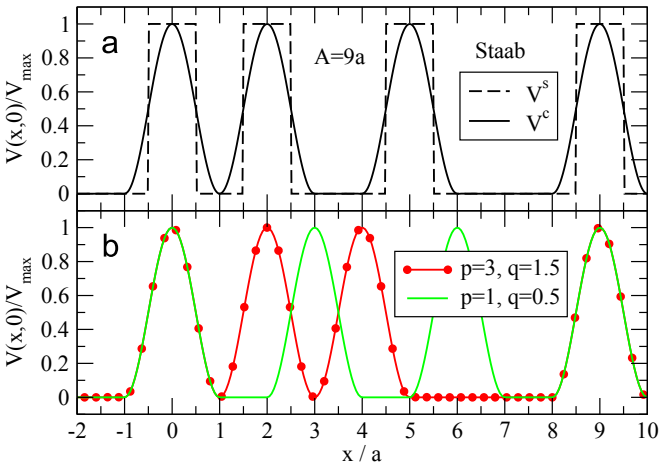

Fig. 1. (a) Periodic potentials without inversion symmetry, Eq. (3), built from the step function $V^s(x)$ and the smooth function $V^c(x)$ of Eq. (2). (b) "Hyperlattice" potentials with inversion symmetry and the same number of building blocks $V^c(x)$ per unit cell as in (a).

$$V^s(x) = V_{max}\ \theta(a - 2|x|), \quad V^c(x) = \frac{V_{max}}{2}[1 + \cos(\pi x/a)]\theta(a - |x|). \tag{2}$$

To describe the modulation with broken inversion symmetry used in [1], we write in the unit cell $-a \le x < 8a$ of width $A = 9a$ the potential

$$V(x, 0) = V_{str}(x, 0) + V_{str}(x - 2a, 0) + V_{str}(x - 5a, 0) \tag{3}$$

and repeat this periodically with period A. Fig. 1(a) shows the result for both the step function and the continuous potential given in Eq. (2) in an interval containing a unit cell.

To model a "hyperlattice" containing p stripes of center-distance $b = 2a$ per unit cell of width $A = (p + q)b$, we write in the unit cell $-a \le x < A - a$

$$V(x, 0) = \sum_{j=0}^{p-1} V_{str}(x - jb, 0) \tag{4}$$

and repeat this periodically with period A. Since $V_{str}(-x, 0) = V_{str}(x, 0)$, these hyperlattice potentials are inversion symmetric with respect to certain x-values. Fig. 1(b) shows two hyperlattice potentials, which contain the same building blocks in the unit cell of width $A = 9a$ as the smooth potential in Fig. 1(a), but at slightly different positions, and we will see that this leads to very different resistance corrections. For $(p, q) = (1, 0.5)$ the cell of width $9a$ contains three unit cells of a simpler lattice with period $2a(p + q) = 3a$.

If we choose $q=0$, for any integer value of $p > 0$, the "hyperlattice" with period $A=pb$ is physically equivalent to the simple lattice with $p=1$ and period $b = 2a$. For $V_{str} = V^c$ this is a simple cosine modulation. Fig. 2 shows such a potential together with three other hyperlattice potentials investigated in [9].

To calculate the resistance corrections caused by such a modulation potential, we need the Fourier coefficients $V_k(0)$ satisfying

$$V(x, 0) = \sum_{k=-\infty}^{\infty} V_k(0)e^{ikKx}, \quad V_k(0) = \frac{1}{A}\int_{-a}^{A-a} dx V(x, 0)e^{-ikKx}. \tag{5}$$

with $K = 2\pi/A$. If this surface potential is an electrostatic potential and if there are no free charges between surface and the 2DES, Poisson's equation requires an exponential damping of the Fourier coefficients with the distance z from the surface, $V_k(z) = V_k(0)\exp(-K|kz|)$. Furthermore the potential $V(x, z)$ will be

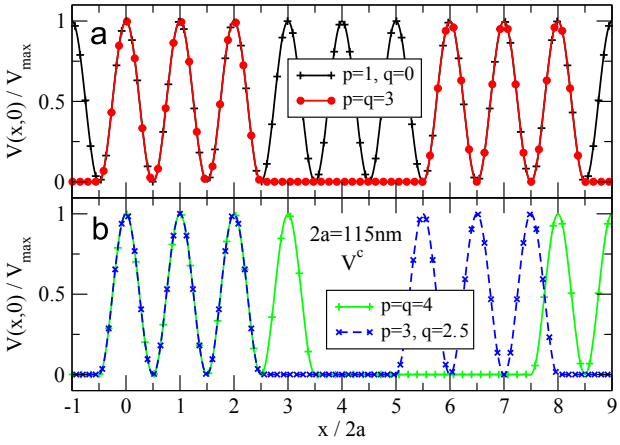

Fig. 2. "Hyperlattice" potentials, Eq. (4), with building blocks $V_{str}(x, 0) = V^c(x)$, for (a) $p = 1$, $q = 0$ and $p = q = 3$ and (b) $p = q = 4$ and $p = 3$, $q = 2.5$.

screened by the 2DES. Since we are interested in small magnetic fields, where Landau quantization and Shubnikov–de Haas oscillations are not resolved, we assume linear screening with the Lindhard dielectric constant $\varepsilon(q) = 1 + 2/(|q|a_B)$, with $a_B = 9.79$ nm the effective Bohr radius of GaAs [13,14]. As a consequence one obtains, in the semiclassical limit of sufficiently low temperatures and magnetic fields [13], for the modulation induced resistance correction

$$\Delta\rho_{xx}^{cl}/\rho_0 = \eta B_{\rm res} \sum_{k=1}^{\infty} k|v_k^{sc}(z)|^2 \cos^2\left(\frac{\pi k}{B_{\rm res}} - \frac{\pi}{4}\right), \tag{6}$$

where $\rho_0 = m/(e^2 n_s \tau)$ is the classical Drude resistance with τ being the transport scattering time, $B_{\rm res} = A/2R_c$ is a rescaled value of the applied magnetic field, $\eta = (4\tau V_{max})^2/(\pi\hbar^2 A^2 n_s)$ contains strength and period of the modulation, and

$$v_k^{sc}(z) = V_k(z)/[V_{max}\,\varepsilon(kK)] \tag{7}$$

are scaled Fourier coefficients, which depend on the spatial structure of the modulation but not on its strength. In the following we will write $\eta = \tilde{\eta}/(A^2 n_s)$ and plot the rescaled resistance correction

$$\Delta\rho_{res} = \Delta\rho_{xx}^{cl}/(\rho_0\tilde{\eta}), \tag{8}$$

which depends only on the shape of the periodic modulation, but not on its strength. If we consider the "hyperlattice" for any positive integer p and $q=0$, and the potential $V_{str} = V^c$, we obtain formally the period $A = 2pa$, the rescaled B-value $B_{res} = pa/R_c$ and non-vanishing Fourier coefficients $V_k(0)$ only for $k=0$ and $|k| = p$. As a consequence in the sum in Eq. (6) only the term with $k=p$ survives and the ratios $B_{res}\,k/(A^2 n_s)$ and k/B_{res} reduce to $(a/R_c)/[(2a)^2 n_s]$ and R_c/a, respectively, i.e. to the values for the simple harmonic potential with $p=1$ and period $2a$, so that the rescaled $\Delta\rho_{res}$ defined in Eq. (8) is the same for all p.

3. Numerical results

3.1. Periodic array without inversion symmetry

3.1.1. Potential and Fourier coefficients

The Fourier components of $V(x, 0)$, Eq. (3), built with the step function of Eq. (2) can be written

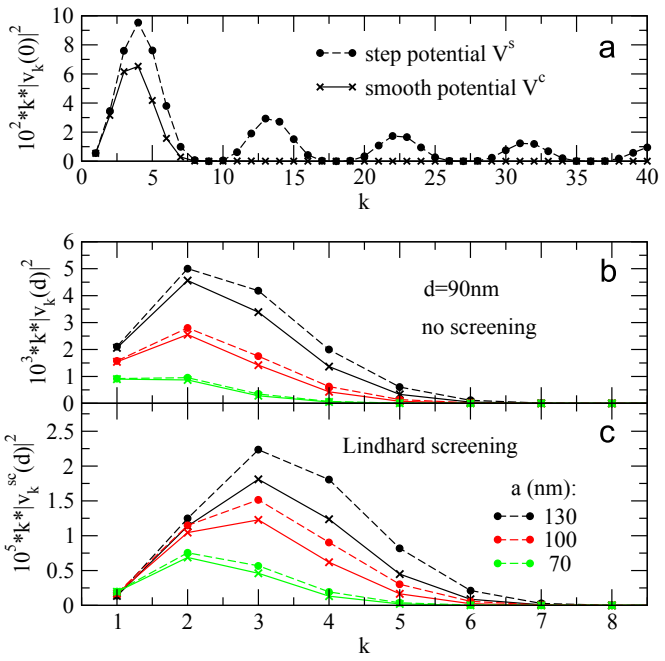

Fig. 3. Weight factors $k|V_k(z)/V_{max}|^2$ of Eq. (6) for modulation by the step potential V^s (filled circles) and by the smooth potential V^c (crosses x) shown in Fig. 1(a). (a) Without screening in the surface plane $z=0$; (b) without screening in the plane $z = d = 90$ nm, $V_k(d) = V_k(0)e^{-2\pi|k|d/A}$, with $A = 9a$; (c) in the plane $z=d$ with Lindhard screening by the 2DES, $V_k^{sc}(d) = V_k(d)/[1 + \pi A/(|k|a_B)]$.

$$\frac{V_k^s(0)}{V_{max}} = \frac{\sin\xi_k}{\pi k}\left(1 + e^{-i4\xi_k} + e^{-i10\xi_k}\right), \quad \xi_k = \frac{\pi k}{9}, \tag{9}$$

with $V_0^s(0) = V_{max}/3$ and $V_{-k}^s(0) = V_k^s(0)^\star$. (This looks simpler than, but is equivalent to, Eq. (6) of [1].) Apparently $V_k^s(0) = 0$ if $k = 9n$ with n being an integer, but which of the coefficients are relevant for the resistance correction? To find this out we plot in Fig. 3 (a) the squared modulus of $V_k(0)$, but in view of Eq. (6) multiplied with k.

We include the corresponding data obtained from the modulation potential built with the smooth function $V^c(x)$ of Eq. (2), leading to the Fourier coefficients

$$\frac{V_k^c(0)}{V_{max}} = \frac{\sin 2\xi_k}{2\pi k[1 - 4k^2/81]}\left(1 + e^{-i4\xi_k} + e^{-i10\xi_k}\right), \tag{10}$$

again with $V_0^c(0) = V_{max}/3$, $V_{-k}^c(0) = V_k^c(0)^\star$, and with $V_{9n}^c = 0$.

According to Eq. (10), for the smooth modulation potential the Fourier coefficients $V_k^c(0)$ with $|k| > 8$ become very small ($\sim|k|^{-3}$), whereas, according to Eq. (9), for the modulation with a step potential the magnitude of the $V_k^s(0)$ with $|k|$ close to $9n + 4$ for integer $n = 0, 1, 2, \ldots$ decreases very slowly ($\sim|k|^{-1}$). This very different behavior of step-like and smooth modulation potential can also be seen from Fig. 3(a). As a consequence, one needs only a few terms ($|k| \lesssim 8$) in order to express the smooth modulation as a sum of its Fourier contributions according to Eq. (5), whereas one gets only a poor, strongly fluctuation approximation to the step-like modulation if one sums even all Fourier contributions with $|k| \lesssim 50$.

This changes drastically, if we consider the electrostatic modulation potential in the plane of the 2DES $d=90$ nm below the surface. Due to the exponential damping, which becomes increasingly important with increasing $|k|$ and with decreasing modulation period A, only the $V_k(d)$ with $|k| \le 5$ remain relevant for the largest modulation period $A = 9a = 1170$ nm considered in [1] and only those with $|k| = 1, 2, 3$ for the smallest considered period $A = 630$ nm, as demonstrated in Fig. 3(b). Lindhard screening by

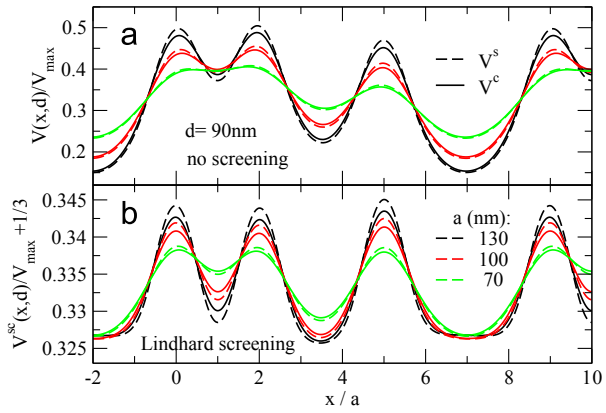

Fig. 4. Poisson-damped potentials of Fig. 1(a) in the plane $z=d$, (a) without and (b) with Lindhard screening by the 2DES, for the indicated stripe widths a, i.e., modulation periods $A = 9a$.

the 2DES suppresses the V_k-values further and is most effective for small $|k|$ and for large A. The contribution with $|k| = 1$ is most strongly suppressed, so that for $A = 630$ nm only the harmonics with $|k| = 2, 3$ remain relevant, whereas for $A = 1170$ nm the most relevant $|k|$-values are 2, 3, 4, and maybe 5, as is shown in Fig. 3(c). These results are qualitatively the same for the step-like and the smooth modulation potential applied in the surface plane.

The effect of Poisson damping and Lindhard screening on the modulation potential itself is demonstrated in Fig. 4.

Fig. 4(a) shows clearly that the exponential damping of higher Fourier components, required by Poisson's equation, becomes more important for arrays with smaller period. Whereas for the period $A = 1170$ nm four Fourier components contribute considerably to the resistance correction, for $A = 630$ nm only two relevant contributions are left. This is modified by the Lindhard screening, which reduces most strongly the contributions with small k, as shown in Fig. 4(b). It is also obvious that the differences between step-like and smooth surface potential become irrelevant sufficiently far below the surface and for sufficiently small ratio A/d.

3.1.2. Modulation correction to the resistance

Fig. 5 shows, for the modulation with broken inversion symmetry and for the parameters used in the experiment [1], rescaled resistance corrections calculated from Eq. (6).

In view of the following discussion the hypothetical case of a 2DES in the surface plane $z=0$ (without screening) is included, Fig. 5(a). For the step-like modulation Fourier coefficients $V_k(0)$ with $|k| \le 50$ are considered, whereas for the smooth modulation and for the results in the plane $z=d$ the consideration of harmonics with $|k| < 6$ is sufficient. Compared with the results for smooth modulation, those for step-like modulation show much larger values and strong fluctuations, which indicates the importance of higher harmonics.

The dependence of the results of Fig. 5(a) on the stripe width a results only from the prefactor $1/A^2$ and would disappear, if $\Delta\rho_{res}$ in Eq. (8) had been defined with η instead of $\tilde{\eta}$ in the denominator. Comparison of Fig. 5(a) and (b) shows that the exponential damping required by Poisson's equation is most effective for the modulation with the smallest period $A = 9a = 630$ nm, and that it strongly reduces the effect of higher harmonics, so that the difference between step-like and smooth surface modulation becomes irrelevant with increasing ratio d/A. Comparison of Fig. 5 (b) and (c) shows that the suppression of the slowly varying lower harmonics by Lindhard screening may enhance the magnetoresistance oscillations due to higher harmonics of the modulation potential.

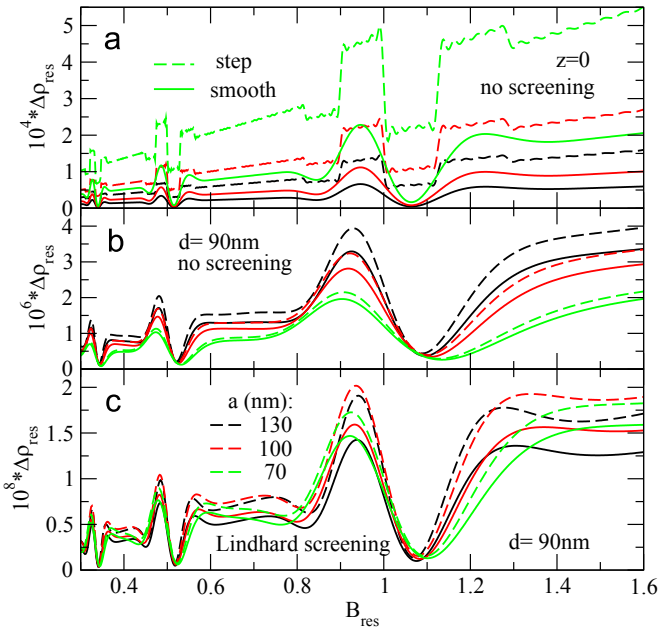

Fig. 5. Rescaled resistance corrections (6) calculated for the indicated stripe widths a and the step-like (broken lines) and the smooth (solid lines) electrostatic surface potential without inversion symmetry. The result in the plane $z=d$ is shown with (c) and without (b) Lindhard screening. The hypothetical result for a 2DES at $z=0$ without screening is shown in (a). (For interpretation of the references to color in this figure caption, the reader is referred to the web version of this paper.)

As explained in [1], up to the prefactor B_{res} the resistance correction $\Delta\rho_{res}$ of Eq. (8) is periodic in $1/B_{res}$ with period 1, and the contribution of the kth harmonic vanishes at

$$B_{res} = \frac{A}{2R_c} = \frac{k}{\lambda - 1/4} =: B_{res}(k, \lambda) \quad \text{for} \quad \lambda = 1, 2, \ldots. \tag{11}$$

Apparently the deep minima of $\Delta\rho_{res}$ in Fig. 5(c) are not well described by Eq. (1), which predicts zeroes at $B_{res}(1, \lambda) = 1.33, 0.57, 0.36, \ldots$ for $\lambda = 1, 2, 3, \ldots$. This is understandable from Fig. 3(c), which indicates that the harmonics with $2 \le k \le 5$ are much more important than the fundamental harmonic with $k=1$. The zeroes of the important harmonics, at $B_{res}(2, 2) = 1.14$, $B_{res}(3, 3) = 1.09$, $B_{res}(4, 4) = 1.07$, and $B_{res}(5, 5) = 1.05$, are located close to each other and explain the pronounced minimum of $\Delta\rho_{res}$ at $B_{res} = 1.1$ for the modulation with period 630 nm, which is dominated by $k=2$ and 3, and at $B_{res} = 1.08$ for the modulations with periods 900 nm and 1170 nm, which are dominated by $k=2$, 3, 4, and 5. Due to the mentioned periodicity in $1/B_{res}$, a zero at $B_{res}(k, k)$ implies a zero at $B_{res}(k, 2k)$, i.e. at $B_{res}(3, 6) = 0.522$, $B_{res}(4, 8) = 0.516$, etc. This explains the minima near $B_{res} = 0.52$ in Fig. 5(c). As has been discussed in [1], these theoretical results explain nicely the positions of minima of the modulation-induced resistance corrections. The detailed B-dependence of the oscillatory corrections is hard to extract from the experiments because of a strong non-oscillating magnetoresistance, which also occurs in the modulated systems and is not considered in the present theory.

3.2. Other symmetries

3.2.1. Importance of stripe positions

So far we have considered a configuration of the three stripes per unit cell of the imposed superlattice, which breaks the inversion symmetry. It is interesting to investigate how the resistance correction is affected by a modification of this configuration. In the following we will consider "hyperlattices" as in Eq. (4), with a unit cell of width $A = (p + q)b$, which contains a series of p neighboring

stripes of center distance $b = 2a$ and an empty region of width qb. The surface potential in the unit cell at $-a \le x \le A - a$ is given by Eq. (4) with the $V_{str} = V^c$ of (2). The Fourier coefficients are $V_0(0)/V_{max} = p/[2(p+q)]$, $V_{p+q}(0)/V_{max} = p/[4(p+q)]$ if $p+q$ is integer, and for all other $k > 0$

$$V_k(0) = \frac{V_{max}\ \sin\left(p\pi k/(p+q)\right)}{2\pi k[1 - k^2/(p+q)^2]} e^{-i\pi k(p-1)/(p+q)}. \tag{12}$$

As a first example we consider the hyperlattice with $p=3$ and $q = 3/2$, shown in Fig. 1(b), i.e. we consider stripes centered at $x=0$, $x = 2a$ and $x = 4a$, which according to Eq. (2) occupy the interval $-a < x < 5a$, and leave the interval $5a < x < 8a$ free of stripes. This is a hyperlattice in the sense of [9] with period $A = 9a$, with inversion symmetry, e.g. around $x_0 = 2a$ and around $x_1 = 6.5a$. Since $p + q = 9/2$ is not integer, we obtain from Eq. (12) the Fourier coefficients $V_0^{hyp}(0) = V_{max}/3$ and

$$V_k^{hyp}(0) = \frac{V_{max}\ \sin(2\pi k/3)}{2\pi k[1 - 4k^2/81]} e^{-i4\pi k/9} \quad \text{for} \quad k > 0. \tag{13}$$

For comparison we also consider the "hyperlattice" with $p=1$ and $q = 1/2$, also indicated in Fig. 1(b), which effectively is a simply periodic lattice with period $A = 3a$ with inversion symmetry, e.g. around $x_0 = 0$, but can also be considered as a lattice with period $9a$, where the unit cell consists of three unit cells of the simple lattice. Describing this as the simple lattice with period $A = 3a$ and with $K = 2\pi/(3a)$, we obtain the Fourier coefficients $V_0^{sim}(0) = V_{max}/3$ and

$$V_k^{sim}(0) = \frac{V_{max}\ \sin(2\pi k/3)}{2\pi k[1 - 4k^2/9]} \quad \text{for} \quad k > 0. \tag{14}$$

Apparently the Fourier coefficients $V_k(0)$ vanish for both models, if k is an integer multiple of 3.

Fig. 6(a) shows these inversion-symmetric potentials, Poisson-damped in the plane $z=d$, in an interval containing a full period $A = 9a$, together with the damped modulation of the same period without inversion symmetry [1]. The effect of both, electrostatic damping and Lindhard screening, is shown in 6(b).

Although the three modulation types presented in Fig. 6 show certain similarities, they lead to rather different resistance corrections. Fig. 7 shows for these three models the corresponding weight factors of the harmonics and the resulting $\Delta\rho_{res}(B)$. Since we generate the modulations from the smooth potential $V^c(x)$, we know from Fig. 3(a) that we need to consider only harmonics with $|k| \le 8$ for the modulation without inversion symmetry. We have checked that this also holds for the other models. In Fig. 7(a)–(c) the

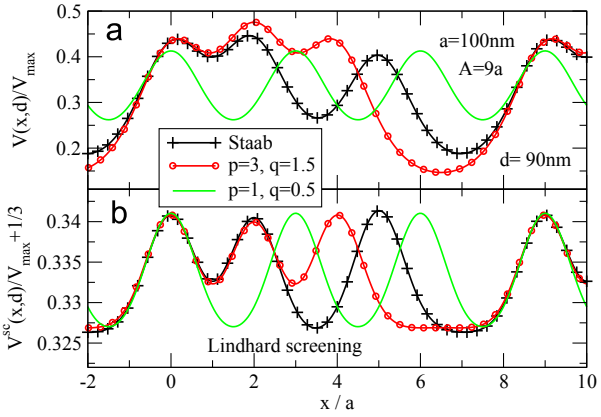

Fig. 6. Smooth modulation potentials as in Fig. 1 (with the same color code), Poisson-damped in the plane $z = d = 90$ nm, (a) without and (b) with Lindhard screening by the 2DES.

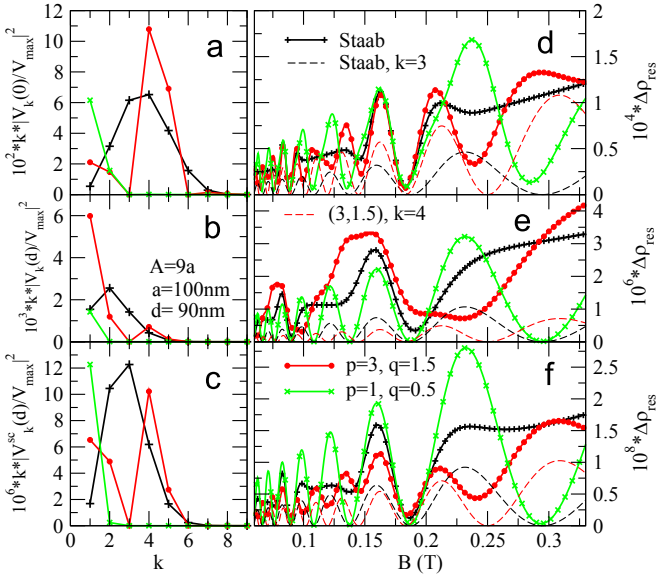

Fig. 7. Resistance corrections due to the smooth modulations of Figs. 1 and 6, (d)–(f), and the weight factors of the relevant harmonics, (a)–(c); (a) and (d) are for a 2DES without screening in the surface plane $z=0$, (b) and (e) for the same 2DES in the plane $z=d$, and (c) and (f) refer to the 2DES at $z=d$ with Lindhard screening. (For interpretation of the references to color in this figure caption, the reader is referred to the web version of this paper.)

data of Fig. 3 for the smooth modulation with $a = 100$ nm are reproduced as black plus signs (+), and the corresponding results for the resistance correction, which were given as functions of B_{res} by the solid red lines in Fig. 5(a)–(c) are shown as functions of the un-scaled magnetic field B by the black solid lines (with black plus signs) in Fig. 7(d)–(f). These results for the modulation with broken inversion symmetry are compared in Fig. 7 with the corresponding results for the hyperlattice modulation $(p, q) = (3, 1.5)$ with the same period, but a different arrangement of the three stripes in the unit cell. The weight factors of the relevant harmonics are indicated by red circles, and the resulting resistance corrections by red lines with red dots. Weight factors for a hypothetical 2DES without screening in the surface plane $z=0$ are given in Fig. 7(a), for the electrostatically damped modulation in the plane $z=d$ in (b), and for the damped and screened modulation in (c). Apparently the harmonics with $k=3$ and 6 do not contribute to this hyperlattice modulation, whereas the harmonic $k=3$ yields an important contribution to the resistance correction (thin broken black lines in Fig. 7(d)–(f)) in the case of the modulation with broken inversion symmetry. To describe the hyperlattice modulation correctly, we need the $V_k^{hyp}(0)$ of Eq. (13) for $k = 1,\ 2,\ 4$ and 5. In Fig. 7(d) and (f) the dominant contribution to the hyperlattice modulation comes from the harmonics with $k=4$, which are shown by the thin broken red lines. In Fig. 7(e) the low harmonics $k=1$ and $k=2$, which are much less damped than $k=4$ and $k=5$, dominate the slow variation of $\Delta\rho_{res}$ with B. However, screening affects the lower harmonics much more than those with larger k-values, and therefore the latter recover in Fig. 7(f), where $k=4$ becomes dominant.

As indicated in Fig. 7(a)–(c) by green crosses (x), we need for the simply periodic modulation the $V_k^{sim}(0)$ of Eq. (14) only for $k=1$ and 2. Since this modulation potential effectively has the period $A_{sim} = 3a$ instead of $A = 9a$, we plot in Fig. 7 the resistance corrections as functions of B instead of B_{res}, and those for the simply periodic modulation as solid green lines (with green crosses). Due to the distance between the equally spaced stripes this modulation potential is not harmonic, and in Fig. 7(a) and (d) a finite contribution of the second harmonic, $k=2$, can be seen. But due to the

small period $A_{sim} = 3a \ll 9a$ the exponential damping of this harmonic with the distance from the surface is much stronger than that with $k=1$, and in Fig. 7(e) and (f) only the fundamental oscillation with $k=1$ survives.

It may be instructive to consider this simple lattice of period $A_{sim} = 3a$ formally as a hyperlattice with period $A = 9a$, with a unit cell containing three neighboring unit cells of the simple lattice. Calculating Fourier coefficients according to Eq. (5) with $K = 2\pi/A$ one obtains $V_0(0) = V_{max}/3$ and

$$V_k(0) = \frac{V_{max}\ \sin(2\pi k/9)}{2\pi k[1-4k^2/81]}\left(1+2\cos(2\pi k/3)\right)e^{-i2\pi k/3} \quad \text{for} \quad k > 0. \tag{15}$$

This yields for any integer n $V_k(0) = 0$ if $k = 3n \pm 1$ and $V_{3n}(0) = V_n^{sim}(0)$, as in Eq. (14). This demonstrates the relevance of the geometrical arrangement of the three stripes in the unit cell of the "hyperlattice" for the importance of the harmonics contributing to the resistance oscillations: symmetric arrangement with equal distance between all neighboring stripes eliminates all harmonics $k \neq 3n$, arrangement of the three stripes in the unit cell next to each other eliminates just the harmonics $V_k^{hyp}(0)$ with $k = 3n$. For the arrangement with broken inversion symmetry, on the other hand, the harmonics with $k = 2, 4$ are of similar importance as that with $k=3$.

3.2.2. *Effect of electrostatic damping*

We now consider hyperlattice modulations with the geometry used by Endo and Iye [9] and build the structures with the smooth potential $V^c(x)$ of Eq. (2) for $b = 2a = 115$ nm. According to Eq. (4) the hyperlattice (p, q) contains in each unit cell an interval of width pb with p periods of the cosine modulation defined in Eq. (2) and an interval of width qb without modulation. Following Ref. [9], we consider $(p, q) = (3, 3)$, $(4, 4)$, and $(3, 2.5)$, and compare these with the simple cosine modulation potential $(1, 0)$. These modulation potentials have been plotted in Fig. 2.

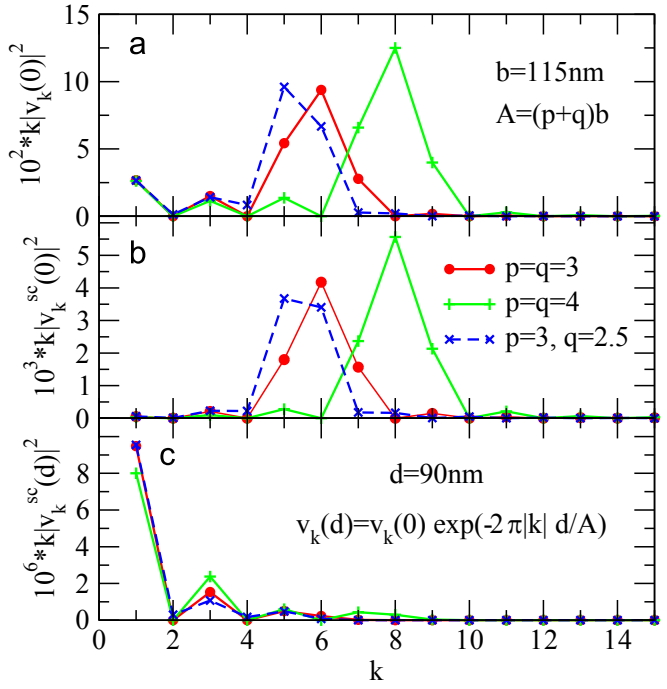

Fig. 8. Weight factors as in Fig. 3 but for the hyperlattices $(p, q) = (3, 3)$, $(4, 4)$, and $(3, 2.5)$. In (a) and (b) modulation and 2DES are assumed to be in the same plane, and in (b) Lindhard screening is considered, in (a) not. In (c) screening and Poisson-damping over the distance d are included.

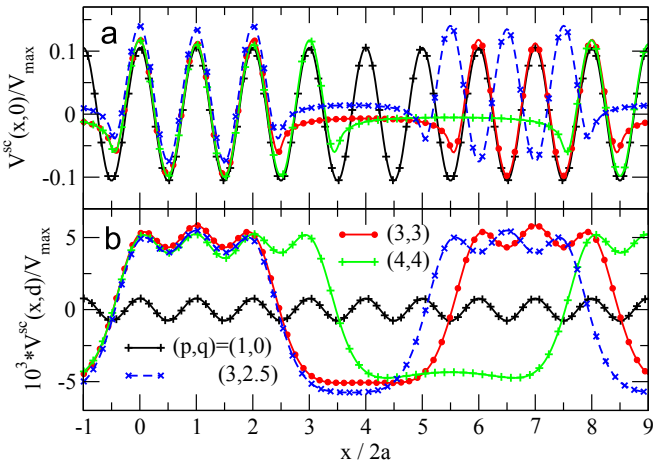

Fig. 9. Lindhard-screened hyperlattice potentials of Fig. 2 (same color code) assuming the electrostatic modulation potential and the 2DES (a) in the same plane, and (b) at a distance $d = 90$ nm, leading to Poisson-damping.

Weight factors, similar to those of Fig. 3, for the hyperlattice potentials, are plotted in Fig. 8 for three situations. In Fig. 8(a) and (b) the modulation potential is assumed in the plane of the 2DES, and the weight factors are calculated in Fig. 8(a) without and in Fig. 8(b) with Lindhard screening by the 2DES. In Fig. 8(c) the modulation is considered as an electrostatic potential in the surface plane $d = 90$ nm above the plane of the 2DES, and the weight factors are calculated considering Poisson-damping and Lindhard screening.

The trivial weight factors for the harmonic modulation with Fourier coefficients $V_0(0) = V_{max}/2$, $V_1(0) = V_{max}/4$ and $V_k(0) = 0$ for $|k| > 1$ are not shown.

Apparently the Poisson-damping suppresses the relevant Fourier contributions to the original modulation potential drastically. This is also seen from Fig. 9, which shows the screened potentials corresponding to the situations of Fig. 8(b) and (c). Due to Poisson's equation, at some distance below the surface the high-frequency oscillations of an electrostatic potential are strongly reduced and only the low-frequency oscillations survive.

Since the hyperlattices under consideration contain periodically sections with the simple cosine oscillation of period b, one might expect to observe the corresponding magnetoresistance oscillations, i.e. oscillations similar to those obtained for the simple cosine modulation. In the experiments [9] this indeed was observed. But if we assume that the modulation produces an electrostatic surface potential of the form as shown in Fig. 2, the exponential damping ($\propto \exp(-dK|k|)$) of higher harmonics leads in the plane of the 2DES, $d = 90$ nm below the surface, to the Lindhard screened potentials shown in Fig. 9(b). For the weight factors of the hyperlattice $(3, 3)$ with $K = \pi/(3b)$ the damping factors $\exp(-2dK|k|)$ are $\exp(-[2\pi/3]90/115) = 0.194$ for $k=1$ and 5.36×10^{-5} for $k=6$, the harmonic which leads to the same oscillation frequency as the simple modulation with period b. If we also consider the reduction of the weight factors by the Lindhard screening, we find that the weight $k|V_k(0)/V_{max}|^2$ shown in Fig. 8 (a) is reduced by a factor 3.6×10^{-4} for $k=1$ and by a factor 2.4×10^{-6} for $k=6$. The resulting weight factors are shown in Fig. 8 (c), and are dominated by the harmonic $k=1$ and the much smaller harmonic $k=3$. The resulting magnetoresistance shows slow variations with tiny modulations due to the $k=6$ harmonic, which have no similarity with the experimental result of [9]. Thus, an interpretation of the experimental modulation in terms of an electrostatic surface potential is not possible. But this is absolutely in agreement with the statements of Endo and Iye [9], who emphasized that their strain-mediated modulation is different from

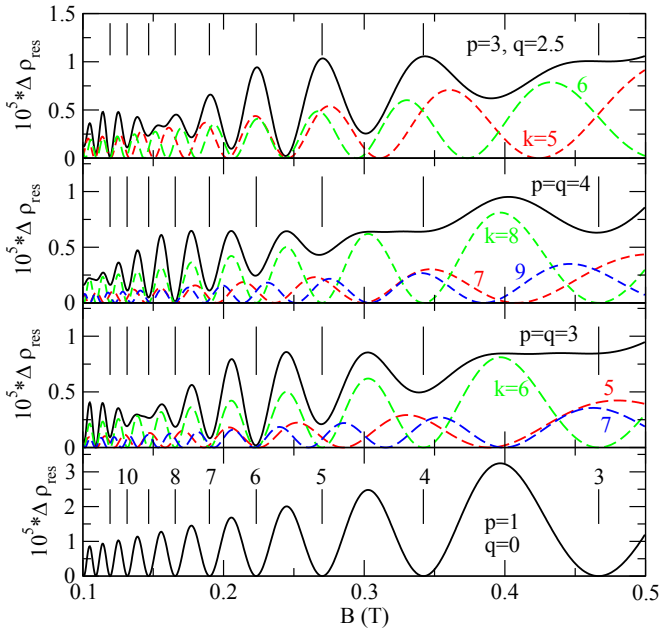

Fig. 10. Rescaled resistance corrections for the simple harmonic modulation with period $b = 115$ nm (lowest panel) and three hyperlattices (p, q), as indicated, with periods $A = (p + q)b$, $n_s 2 \times 10^{11}$ cm^{-2}. For the hyperlattices the dominant harmonic contributions are indicated by broken colored lines. (For interpretation of the references to color in this figure caption, the reader is referred to the web version of this paper.)

an electrostatic one.

Therefore, we make the assumption that the strain-induced modulation can be described by a potential in the plane of the 2DES, which has essentially the form as shown in Fig. 2. Thus we assume that the relative magnitude of the Fourier coefficients in the plane of the 2DES is so as we previously assumed for the electrostatic surface potential. (About the absolute values, i.e. about V_{max}, we make no assumption.) Then, taking Lindhard screening into account, we get the screened potentials and the corresponding weight factors as shown in Figs. 9(a) and 8(b), respectively. Now the weight factors for the hyperlattice (3, 3) are dominated by $k=6$ and those for (4, 4) by $k=8$. The resulting resistance oscillations are shown in Fig. 10. The lowest panel shows the result for the simple harmonic modulation with period $b = 115$ nm and the minima follow Eq. (1) with $\lambda = 3, 4, 5, \ldots$ as indicated. The results for the three hyperlattices compare very nicely with the experimental results of Endo and Iye [9]. The main differences are that in the experiment the oscillations are damped at small B-values, where the cyclotron diameter becomes comparable with the mean free path, and that apparently some experimental results show non-oscillatory magnetoresistance effects. Such effects and collision damping are not included in the present theory. The result for $p = q = 3$ reproduces characteristic features of the experiment: most minima coincide with those described by Eq. (1), but those for $\lambda = 3$ and $\lambda = 9$ are missing. The reason is obviously that near the $\lambda = 3$ minimum at $B = 0.467$ T of the dominant $k=6$ harmonic, which oscillates as a function of B with the same phase as the simple modulation of the lowest panel, the next important harmonics $k=5$ and $k=7$ show maxima. Due to the mentioned periodicity of Eq. (6) in $1/B_{res}$ with period 1, for $k=6$ the situation near $B_{res}(k, \lambda) = k/(\lambda - 1/4)$ with $\lambda = 9$, i.e. near $B = 0.147$ T, is similar to that for $\lambda = 3$.

For $p = q = 4$ we get similar results, but now the leading harmonic is $k=8$ and near its minima for $\lambda = 4$ and $\lambda = 12$ the next important harmonics $k=7$ and $k=9$ show maxima. For $(p, q) = (3, 2.5)$ we find maxima instead of minima for $\lambda = 4, 5, \ldots, 8$, but again minima at $\lambda \geq 9$, also in agreement with the experiment. Since now the period $A = 5.5b$ is not an integer multiple of b, there is no harmonic with the same phase as the modulation in the lowest panel of Fig. 10, and the dominating contributions come from $k=5$ and $k=6$.

4. Summary

We have applied the semiclassical formula of [13] for the magnetoresistance oscillations of a 2DES, modulated by a lateral superlattice with several harmonics, to two types of experiments [1,9], which investigated different types of modulations. Staab et al. [1] produced an electrostatic surface potential by a periodic array of parallel metal stripes with three stripes per unit cell, arranged in such a way that the modulation potential had no inversion symmetry. We have demonstrated that the finite distance between the 2DES and the electrostatic surface potential leads to a strong damping of its higher Fourier coefficients, so that for the resulting resistance oscillations the detailed shape of the potential peaks (step-like or smooth) is not important, as shown in Fig. 5. The position of the potential peaks, produced by the metal stripes, within the unit cell is, however, very important, as seen from Figs. 6 and 7. Unfortunately the experimentally observed resistance oscillation was superimposed by strong non-oscillatory magnetoresistance effects, and only a few oscillation minima could be safely determined. These minima are nicely explained by the calculations and result from the fact that zeros of the most important harmonics at these magnetic fields nearly coincide [1].

In the second type of experiment [9] surface stripes of calixarene resist have been used to produce a strain-mediated lateral "hyperlattice" as modulation of the 2DES. We assumed that each of these stripes produces in the plane of the 2DES a smooth potential peak, and that the center distance of these peaks coincides with the center distance of the surface stripes. Considering the superposition of these potential peaks as periodic hyperlattice, we calculated the induced magnetoresistance oscillations and could reproduce many details of the experimental findings.

It might be interesting to produce modulations with broken inversion symmetry by the method of [9], with the hope to resolve more details of the resulting magnetoresistance oscillations than could be resolved for the modulation by an electrostatic surface potential. This would allow a more detailed comparison with the theory.

Acknowledgements

It is my pleasure to thank Dieter Weiss for informing me about the experiments [1] performed in his group, for renewing my interest in this field of magnetotransport, and for the pleasant cooperation.

References

[1] M. Staab, M. Matuschek, P. Pereira, M. Utz, D. Schuh, D. Bougeard, D. Weiss, R.R. Gerhardts, New J. Phys. 17 (2015) 043035.
[2] M. Staab (Diploma thesis), Universität Regensburg, Inst. II f. Exp. u. Angew. Physik, 2012.
[3] P. Olbrich, E.L. Ivchenko, R. Ravash, T. Feil, S.D. Danilov, J. Allerdings, D. Weiss, D. Schuh, W. Wegscheider, S.D. Ganichev, Phys. Rev. Lett. 103 (2009) 090603.
[4] P. Olbrich, J. Karch, E.L. Ivchenko, J. Kamann, B. März, M. Fehrenbacher, D. Weiss, S.D. Ganichev, Phys. Rev. B 83 (2011) 165320.
[5] E.L. Ivchenko, S.D. Ganichev, JETP Lett. 93 (2011) 673.
[6] D. Weiss, K. von Klitzing, K. Ploog, G. Weimann, Europhys. Lett. 8 (1989) 179.
[7] R.R. Gerhardts, D. Weiss, K. von Klitzing, Phys. Rev. Lett. 62 (1989) 1173.
[8] R.W. Winkler, J.P. Kotthaus, K. Ploog, Phys. Rev. Lett. 62 (1989) 1177.

[9] A. Endo, Y. Iye, J. Phys. Soc. Jpn. 69 (2000) 3656.
[10] V. Vasilopoulos, F.M. Peters, Phys. Rev. Lett. 63 (1989) 2120.
[11] C. Zhang, R.R. Gerhardts, Phys. Rev. B 41 (1990) 12850.
[12] C.W.J. Beenakker, Phys. Rev. Lett. 62 (1989) 2020.
[13] R.R. Gerhardts, Phys. Rev. B 45 (1992) 3449.
[14] J. Labbé, Phys. Rev. B 35 (1987) 1373.